



TRANSVERSE ENERGY PHYSICS WITH THE CDF CALORIMETER\*

J. Freeman, R. Perchonok, and J. Yoh

August 1984

\*Presented at the 4th Topical Workshop on  $p\bar{p}$  Collider Physics, Bern, Switzerland, March 5-8, 1984.

## ABSTRACT

We have studied CDF's ability to measure missing transverse energy and to reconstruct the mass of the  $W \rightarrow 2$  jet system by use of a QCD Monte Carlo and a detailed simulation of the CDF detector.

For monojet events and events with multiple jets and large missing  $E_T$ , we have studied backgrounds from "old physics sources" ( $Z \rightarrow 2\nu$  and heavy quark jets) and from detector mismeasurement. These backgrounds are found to be comparable.

For  $W \rightarrow 2$  jets, we find that the mass resolution is dominated by the ability to discern between particles from  $W$  decay and the underlying event. CDF detector mismeasurement causes only a small deterioration in mass resolution.

## INTRODUCTION

The present era of high energy hadron colliders has opened up an entirely new mass region for the exploration of physics phenomena. New massive objects or phenomena are expected to manifest themselves by their decays into "partons" - electrons, muons, jets (quarks or gluons) and missing  $E_T$  (neutrinos, photinos, etc.). In 1986, the Fermilab Tevatron Collider will bring a four-fold increase in energy and accessible mass range above that presently available.

In this paper, we address the ability of the CDF detector at Fermilab to measure jets and isolate missing  $E_T$ . Our study employs a realistic Monte Carlo simulation including QCD effects and detector imperfections such as cracks, dead areas, shower leakages, and nonuniformities.

CDF's ability to detect missing  $E_T$  physics is studied for two extreme cases of event topology - (i) the loose signature of multijet events with large missing  $E_T$ , and (ii) the tight signature of monojet events, where no energetic cluster is allowed opposite an observed high  $p_T$  jet. For the multijet/large missing  $E_T$  events, we determine that the background from detector mismeasurement of jets is comparable to that due to neutrinos and/or muons from heavy quark jet decays. (This rate is comparable to the signal expected from gluinos). Both the "detector" and the heavy quark backgrounds can be reduced by a factor of 3-5

using additional vetos such as muon and electron tagging or by determining that a high  $p_T$  charged particle has entered a "crack" in the calorimetry. The dominant "old" physics backgrounds for monojet events are the events with a jet recoiling against a  $Z_0$  which decays into two neutrinos or events with heavy quark cascades into neutrinos. The level of this background is about two orders of magnitude below the multijet/large  $E_T$  miss. We find that the "detector" background arising from completely missing a leading jet to be comparable to the jet +  $Z_0$  background.

The accuracy of jet energy determination was studied by determining the mass resolution of events with  $W \rightarrow ud$ . We find that the dominant factor in mass resolution is due to clustering - i.e. the difficulty in determining which particles come from the jets from W decay and which come from the underlying event ("beam-jets"). This factor dominates the detector energy resolution or mismeasurement, suggesting that improvements in resolution (such as using Uranium) or uniformity (such as reducing cracks) will not lead to significant improvements in W mass resolution.

#### CDF CALORIMETRY

The CDF detector is a  $4\pi$  calorimeter which covers  $2^\circ$  to  $178^\circ$  in polar angle (relative to the beam axis) and full  $360^\circ$  coverage in azimuthal angle. It has a projective tower geometry with electromagnetic shower counters surrounded by hadron calorimetry. The detector has a thickness of 108 centimeters of iron equivalent at  $\theta = 90^\circ$  (5.1 absorption lengths), increasing to 160 cm of iron equivalent (7.6 absorption lengths) in the forward direction. The central region ( $\theta$  between  $40^\circ$  and  $140^\circ$ ) contains scintillator plastic sampling calorimetry with  $12\%/\sqrt{E}$  ( $65\%/\sqrt{E}$ ) resolution for the electromagnetic (hadronic) component. The remaining solid angle is covered by proportional tube sampling calorimetry with a resolution of  $25\%/\sqrt{E}$  ( $100\%/\sqrt{E}$ ) electromagnetic (hadronic).

#### CDF SIMULATION

An extensive simulation of the CDF detector has been utilized for the analysis reported in this paper. The physics events of interest are first generated via the ISAJET Monte Carlo.<sup>(1)</sup> After smearing the production vertex ( $\sigma_z = 30$  cm), the events are processed by a geometrically detailed detector simulation (eg. cracks and dead areas in the calorimetry are included).

Physical processes such as in flight decays, gamma conversions,  $dE/dx$ , and multiple scattering are included. Hadronic and electromagnetic showers are simulated including effects such as transverse and longitudinal shower profile fluctuations, energy leakage, and noninteracting punchthrough. Differences in response to electromagnetic and hadronic showers measured at test beam energies were also incorporated in the simulation.<sup>(2)</sup>

#### LACK OF CALORIMETRY AT VERY SMALL FORWARD ANGLES

To find the effect of limited coverage of calorimetry for small polar angle (the half angle of the conical hole in the calorimetry is  $2^\circ$ ), we studied hard scattering events with minimum parton  $p_T > 15$  GeV and  $> 50$  GeV; these partons are allowed to evolve into one or more final state jets according to probability of QCD final state bremsstrahlung. We looked at the final state particles and calculated the magnitude of the missing  $E_T$  vector for various assumptions about the limit of forward calorimetry coverage. Results are shown in Fig. 1A and B. In each of the figures, we see three curves: "No smearing" which shows the effect of the hole considering only geometry with no energy resolution smearing; " $\sigma_E = .55 \sqrt{E}$ ",<sup>(3)</sup> where the no smearing curve is smeared by intrinsic calorimetry resolution; and finally, "CDF uncorrected" which contains all cracks and nonuniformities in CDF, as well as the effect of neutrinos and noninteracting punchthrough, but where no correction for these effects is made. From Fig. 1A, we see a "knee" in the distributions for a hole of  $2^\circ$ . As the size of the hole is increased above that, it becomes probable for one of the 15 GeV  $p_T$  jets to flow into the hole region. Consequently, the missing  $E_T$  resolution worsens. Kinematics constraints force the probability of a jet flowing into the forward direction to decrease with increasing jet transverse energy. Hence, in Fig. 1B, for 50 GeV  $E_T$  jets, we see that the knee for worsening  $E_T$  resolution has moved upward to about  $5^\circ$ . We conclude that for hard scatterings of more than 15 GeV  $E_T$  per parton, the  $2^\circ$  hole in the CDF calorimetry does not contribute to missing  $E_T$  resolution.

#### BACKGROUND FOR MISSING $E_T$ + JETS

It is possible for conventional hard scattering events to be observed possessing missing  $E_T$ . Causes for missing  $E_T$  in these events include semi-leptonic decays of heavy quark jets and detector imperfections. To study the relative importance of different contributing factors, we looked at events

of the process  $p\bar{p} \rightarrow 2 \text{ jets}$ , with  $p_T$  (parton)  $> 50 \text{ GeV}$   $p_T$ . The results obtained from a sample of 1700 events are plotted in Fig. 2. In this figure, we see distributions of  $1/N \text{ dN/d}E_{T\text{missing}}$  versus  $E_T$  missing for the event sample with various analyses applied.

The curve "2<sup>o</sup> hole only" shows the effect of the lack of calorimetry coverage in the very forward direction. Perfect energy resolution is assumed.

Next we see three sets of distributions ("before lepton veto" and "after lepton veto"). The set of distributions "after lepton veto" are considered below. First, consider the curve  $\mu, \nu$  only. This distribution shows the contribution of neutrinos and muons due to weak decays. All energy carried by neutrinos is assumed lost, muons contribute minimum ionizing energy, and otherwise perfect resolution is assumed. We note that the normalization of this curve is the same as the other 2 "before veto" distributions. There is a large spike at missing  $E_T$  equal to zero from events with no neutrinos that is not shown.

The missing  $E_T$  distribution for an "ideal" detector with a 2<sup>o</sup> hole in calorimetry coverage, gaussian energy resolution of  $0.55/\sqrt{E}$ , and with no  $\nu$  or  $\mu$  detection is shown, labelled as ".55/ $\sqrt{E}$  +  $\mu, \nu$ ". We see that, for  $E_T$  missing greater than 20 GeV, this curve asymptotically approaches the curve of  $\mu, \nu$  only. We conclude that intrinsic calorimetry resolution is not a contributing factor in the observation of events with very large missing  $E_T$ .

(Although the curve is not shown, the distribution for an ideal detector with pure gaussian energy resolution of  $0.55/\sqrt{E}$ , able to detect and correct for all neutrinos and muons, follows the curve ".55/ $\sqrt{E}$  +  $\mu, \nu$  after veto" up to  $E_T$  missing of 20 GeV.)

The curves with open squares and triangles in Fig. 2. represent the distribution of  $\mu, \nu$  only and .55/ $\sqrt{E}$  +  $\mu, \nu$  in which events with a charged lepton of momentum greater than 2 GeV were removed. This veto on events with "identifiable" leptons causes a reduction of about 5-10 in the rate of events with large missing  $E_T$ . The actual reduction factor obtained by applying this veto to real data may be less due to inefficiency in tagging (for instance losses due to overlaps) or failure in identification (especially just above the 2 GeV threshold, or at small angles).

We have also investigated the difference in response between electromagnetic and hadronic showers as well as the non-linear momentum dependence for charged hadrons. Fig. 2 contains a curve, labelled

$.55/\sqrt{E} + \mu, \nu + E/H$ , which in addition to the  $2^\circ$  degree hole in calorimetry,  $.55/\sqrt{E}$  smearing, and mismeasurement of muons and neutrinos, we added the following two effects:

(1) The observation that energy deposition by charged hadrons in electromagnetic calorimetry is measured to have a gain that is a factor of 1.4 less than electrons; thus, a 30 GeV pion that leaves 15 GeV in the electromagnetic calorimeter and 15 GeV in the hadronic will have a total reconstructed energy of only 26 GeV since the reconstructed electromagnetic energy is only  $15 \text{ GeV} / 1.4 = 11 \text{ GeV}$ . Note that if the charged pion leaves much more than half of its energy in the front, it must have showered with a large number of pi-zeros produced and thus have reconstructed energy closer to the actual energy deposited. The parameterization of this effect has been extracted from test beam data at 30 GeV in a real prototype CDF calorimetry module.<sup>(2)</sup> (This smearing due to response variation can be corrected for by applying an energy correction dependent on the ratio of observed response in the electromagnetic vs. the hadronic calorimeter. For isolated particles, this correction factor can be as large as 20%. However, due to the statistical nature of jet fragmentation, the maximum correction factor for jets is only 4%. Since the correction for jets is so small, it was ignored throughout this paper. Jet energies were calculated using the linear sum of electromagnetic plus hadronic calorimeter responses.)

(2) UA1 and UA2 have both measured the effect that a 2 GeV charged pion gives less than 1/10 the signal of a 20 GeV charged pion.<sup>(4,5)</sup> A possible explanation of this effect is that lower momentum charged pions give a larger fraction of their energy into nuclear interaction losses which are unobserved. We have parameterized this low energy behavior, using the UA1 data which exhibits almost twice the non-linearity as the UA2 data, yielding in the worst case, for the energy range of 1.35 to 2.6 GeV, a response that is 0.73 of that expected from linear extrapolation from higher energy. The inclusion of these two additional effects appear to cause a 15% deterioration in missing  $E_T$  resolution.

The curve "CDF-before veto" shows the rate expected from the detector simulation for missing  $E_T$  events. (The full CDF simulation is described in a previous section.) No attempt is made to veto events that have particles hitting cracks, identifiable leptons, etc. Due to lack of data, the current CDF detector simulation does not yet include the low energy charged hadron

non-linearity. However, even with the more pessimistic UA1 response, it appears that low energy non-linearity would lead to at most a small (of order 5 %) deterioration in missing  $E_T$  response.

We note that the "CDF-Before lepton veto" distribution also approaches the  $\mu, \nu$  only distribution for missing  $E_T$  greater than 25 GeV. Events that populate the region  $E_T$  missing less than 10-15 GeV are caused predominately by intrinsic calorimetry resolution. To understand the events in the intermediate region of  $E_T$  missing between 15 and 25 GeV, we looked at all events with  $E_{T\text{missing}} > 15$  GeV to find out the cause of missing  $E_T$ . There were three causes for the missing  $E_T$ : Cracks in the calorimetry, intrinsic calorimetry resolution, and neutrinos. Table 1 shows the number of events for each cause.

Table 1

Number of Events/Cause for Events with Missing  $E_T > 15$  GeV

<u>Cause</u>	<u>CDF-Before Veto</u>	<u>After Veto</u>	<u>Veto and Crack Instrumentation</u>
Particles hitting cracks	25	6	1
Intrinsic resolution	14	8	8
Neutrinos	17	4	4

We found that some of the events in the high missing  $E_T$  tail could be vetoed. These events possessed high  $p_T$  charged particles hitting cracks, or identifiable leptons associated with neutrinos. We assumed optimistically that we could identify all charged leptons with energy greater than 2 GeV. Vetoing these events brought about a factor of 3-5 reduction in the high tail. These are the "after lepton veto" distributions in Fig. 2. The relative distribution of causes of missing  $E_T$  events in the high tail changed after the veto. The new balance of causes is shown in Table 1. We see that intrinsic resolution becomes more important as a contribution. We note that the events with missing  $E_T$  caused by intrinsic resolution tend to cluster at the 15 GeV  $E_T$  missing boundary.

A proposed upgrade to CDF would instrument the inactive regions between calorimetry modules in the central region with 7 radiation lengths of converter followed by a single sampling chamber.<sup>(6)</sup> This instrumentation would allow the flagging of events with high energy photons that hit these cracks. If we apply this final rejection, we are left with the third set of numbers in Table 1. We

see that the intrinsic calorimetry resolution has become the predominant cause of the high tail.

For events of the signature 50 GeV  $E_T$  jets with missing  $E_T$  between 15 and 25 GeV, CDF's calorimetry resolution seems to lead to backgrounds twice as severe as the heavy quark background. A thicker calorimeter with better resolution (for example, liquid-Argon/Uranium) could conceivably get 1/3 the background CDF can expect. For higher missing  $E_T$  events, neutrinos become more important as a source of the high missing  $E_T$  tail. Events with missing  $E_T$  greater than 25 GeV are expected to be caused almost solely by neutrinos. It is also worth noting that the missing  $E_T$  vector caused by calorimetry mismeasurement will point along a jet direction, for events with 2 back-to-back jets (the dominant topology). It can be demonstrated that the missing  $E_T$  background caused by intrinsic calorimetry resolution can be removed by a simple topology cut: requiring the missing  $E_T$  vector to point more than  $20^\circ$  azimuthally away from the direction of either of the two leading jets eliminates this background.<sup>(7)</sup>

#### BACKGROUND FOR MONOJET EVENTS

One possible signal for the presence of supersymmetric particles is the observation of "monojet" events. These are events containing a single observable jet and missing transverse energy. Sources of background to supersymmetric monojet events include production of  $g + Z_0(+\nu\nu)$ , cascade decays of heavy quarks, and detector dependent effects such as finite energy resolution, cracks, and non-uniformities, which causes a jet to not be observed. The existence of a 30 GeV mass scalar quark could produce events with a 20 GeV  $E_T$  jet, without a second jet to balance transverse energy. We have studied events with the monojet signature: A cluster with transverse energy equal to or greater than 20 GeV  $E_T$  with less than 5 GeV  $E_T$  balancing the jet in the opposite hemisphere.

Our clustering procedure was:

1) Require a 1 GeV  $E_T$  deposition in a  $15^\circ(\phi) \times 0.1$  (pseudorapidity) tower.

2) Look at all neighbor towers, and add their energy to the cluster if there is at least 0.1 GeV  $E_T$  but less than 1.5X the parent tower's energy in the tower. The last requirement prevents merging of close but distinct clusters. This process was repeated until no new towers could be added to the cluster.

3) Merge all clusters whose centroids are less than 1 unit apart in (pseudorapidity-phi) space, where phi distances are measured in radians. We picked the distance of 1 unit for cluster merging after a hand scan of energy flows for a sample of the events.

We studied 60,000 events of the process  $p\bar{p} \rightarrow \text{jets}$  with  $P_T$  of each parton  $> 30$  GeV. After very loose precuts to eliminate events that could not possibly satisfy our monojet criterion, we simulated the remaining 1500 events using the detailed CDF detector simulation and applied our mono-jet selection. 11 events satisfied the signature. We then identified the source of missing  $E_T$  for these 11 events. There are three sources of missing  $E_T$ : 5 events with a high energy  $\nu$  from heavy quark decay; 3 events with photons hitting the phi cracks between elements of calorimetry in the central region; and 3 events caused by other calorimetry imperfections including finite thickness and limited theta coverage.

One of the five events caused by neutrinos was recognizable as a weak decay event. (It had a 5 GeV  $P_T \mu$  that was detectable.) The remaining four events had very low energy leptons associated with the neutrinos. All of the events due to missed photons could be tagged if CDF adopted the proposal to instrument the cracks in the central calorimetry. None of the events due to other properties of the calorimetry were recognizable as being caused by the detector. Hence, we are left with 4  $\nu$  events and 3 events due to detector limitations. The  $Z_0 + \text{jet}$  source of background would contribute about 2 events.<sup>(1)</sup>

We repeated the analysis for a sample of 80,000 events with parton  $E_T$  greater than 50 GeV. We looked for the monojet signal:  $E_T \text{ jet} > 40$  GeV, with less than 5 GeV  $E_T$  balancing the jet in the opposite phi hemisphere. Of the 80,000 events, we found none that satisfied our criterion. At this energy, the  $g+Z_0$  background would contribute about 5 events.<sup>(1)</sup>

We conclude that CDF calorimetry imperfections generate a background to monojet events which is comparable to or less than the physics background of  $Z_0 + \text{jets}$  or heavy quark decay. In other words, a perfect calorimeter would not have a significantly lower background for monojet events caused by supersymmetry.

#### MASS RESOLUTION OF $W \rightarrow u\bar{d} \rightarrow 2 \text{ Jets}$

We studied CDF's ability to reconstruct the invariant mass of a 2 jet system by considering the process  $W \rightarrow u\bar{d} \rightarrow 2 \text{ jets}$  for the cases of the mass of the W at the measured value of 80 GeV, and a hypothetical heavy W with  $M_W$  of 500

GeV. Our method of analysis was to first identify the factors contributing to finite mass resolution. We then added each factor to our sample of simulated events and observed the effect on the measurement. The effects we identified as interesting to study were:  $2^\circ$  hole in calorimetry; energy lost by neutrinos and muons; intrinsic calorimetry resolution; calorimetry imperfections, such as finite thickness, cracks, and non-uniformity; and the effects of clustering algorithms used to reconstruct the fragmented jets.

A summary of our conclusion is shown in Table 2. Distributions E - H show the effects of a realistic clustering algorithm. For distributions A - D, a priori knowledge of the parent partons of the final state particles was used to reconstruct the jets. We note that the same clustering and cluster-merging algorithms described in the section on monojet identification were used in this analysis. For the case of  $M_W=80$  GeV, several mass distributions for sets of conditions A through H are shown in Figs. 3 and 4.

In Fig. 3, we see results for: C, ".25/  $\sqrt{E}$  ideal clustering", an ideal liquid-Argon/Uranium calorimeter with a priori knowledge of which particle belongs to which jet (hence, ideal clustering); D, ".55/  $\sqrt{E}$  ideal clustering", an ideal conventional calorimeter without the effects of realistic clustering; and F, ".25/  $\sqrt{E}$  realistic clustering", the ideal U-1A calorimeter, after the effect of realistic clustering. We observe that the .25/  $\sqrt{E}$  calorimeter, after clustering, has poorer resolution than the .55/  $\sqrt{E}$  calorimeter before clustering. In Fig. 4, we see results for cases: F, again the .25/  $\sqrt{E}$  calorimeter after clustering; G, the .55/  $\sqrt{E}$  calorimeter after clustering; and H, CDF including all cracks, nonuniformities etc., after clustering. From Fig. 4, we conclude that there are no dramatic differences between distributions F, G, and H.

For low mass objects ( around 80 GeV ) that decay into two jets, we found that clustering techniques are the dominate source of degraded mass resolution. Improved calorimetry resolution does not cause a significant improvement in mass resolution. The effect of calorimetry resolution becomes more important for heavier mass objects (e.g. 500 GeV), where the decay jets are unambiguous. After clustering, the resolution of CDF is about 1.6 times worse than that of an ideal liquid-Argon/Uranium detector, as compared with 1.3 times worse at a mass of 80 GeV. Note that improved CDF mass resolution is expected through veto of events with mismeasured energy flagged by energy leakage into cracks, or large missing  $E_T$ . In addition, the liquid-Argon/Uranium resolution is expected to

worsen due to effects of calorimetry calibration, which were not accounted for in this analysis.

Table 2

Factors contributing to degraded mass resolution in  $W \rightarrow 2$  jets.

<u>Factor</u>	<u><math>\sigma</math> Resolution (<math>M_W=80\text{GeV}</math>)<sup>*</sup></u>	<u><math>\sigma(M_W=500\text{GeV})</math><sup>*</sup></u>
A. $2^\circ$ beam hole	0.6%	.5%
B. A + missing $\nu, \mu$	1.3%	1.0%
C. B + $.25/\sqrt{E}$ resolution	3.0%	1.5%
D. B + $.55/\sqrt{E}$ resolution	5.3%	2.2%
E. B + clustering	7%	2.4%
F. C + clustering	8%	3.0%
G. D + clustering	9%	3.9%
H. CDF	10%	4.9%

\* $\sigma$  is defined using only the 50%-80% interval of the relevant distribution. Events were entered into distributions E through H only if they possessed at least 2 clusters, each with  $E_T > 15$  GeV.

### CONCLUSIONS

CDF was designed to serve as a full  $4\pi$  calorimeter with homogenous response. Some compromises were necessary in order to realize the design. The cracks and nonuniformities in the calorimetry are attributable to the requirement of modularity, coupled with the necessity of reading out the signals. Finite calorimetry thickness, and limited solid angle coverage are forced upon one by geometrical constraints. We found that these imperfections will not seriously detract from our ability to study jets and missing  $E_T$ . For many of the processes studied, CDF's imperfections cause only insignificant degradations to the best achievable resolution, and in the worst case, these imperfections create a background that is comparable to the intrinsic background from physics processes.

REFERENCES

1. F. E. Paige and S. D. Protopopescu, 1982 DPF Summer Study, Snowmass, Co., June 28, 1982, page 471.

We used ISAJET version 4.0 for these studies. The ISAJET event generator does not contain the effects of initial state gluon bremsstrahlung. For the studies presented in this paper, initial state bremsstrahlung is expected to be several orders of magnitude less important than the other effects studied, and is consequently ignored.

2. CDF internal note number 115

3. Throughout this paper, we consider two "ideal" detectors: a "conventional" calorimeter, and a "liquid-Argon/Uranium" calorimeter. These calorimeters have finite energy resolution ( $\sigma/E = 0.55/\sqrt{E}$  for the conventional one;  $0.25/\sqrt{E}$  for LA-U), and infinite thickness. They also have perfect spatial resolution and no difference in response to electromagnetic and hadronic showers. The conventional calorimeter energy resolution was determined by averaging the electromagnetic and hadronic calorimeter response expected by CDF over a sample of hard scattering events. The same averaging was done with the liquid Argon/Uranium ideal detector, using as input resolutions  $0.1/\sqrt{E}$  for electromagnetic calorimetry and  $0.35/\sqrt{E}$  for hadronic.

4. M. J. Corden, et al., Physica Scripta. Vol. 25, 1982, page 5.

5. A. Beer, et al., CERN-EP/83-175.

6. CDF internal note number 225

7.  $P_{OUT}$  cuts have been studied, and are useful in eliminating the hard scattering background from the signal of supersymmetric particles. See for example:

S. H. Aronson, L. S. Littenberg, F. E. Paige, 1982 DPF Summer Study, Snowmass, Co., June 28, 1982, page 505.

CDF internal note 227.

We expect that in analyses for supersymmetry, a  $P_{OUT}$  cut will be necessary.

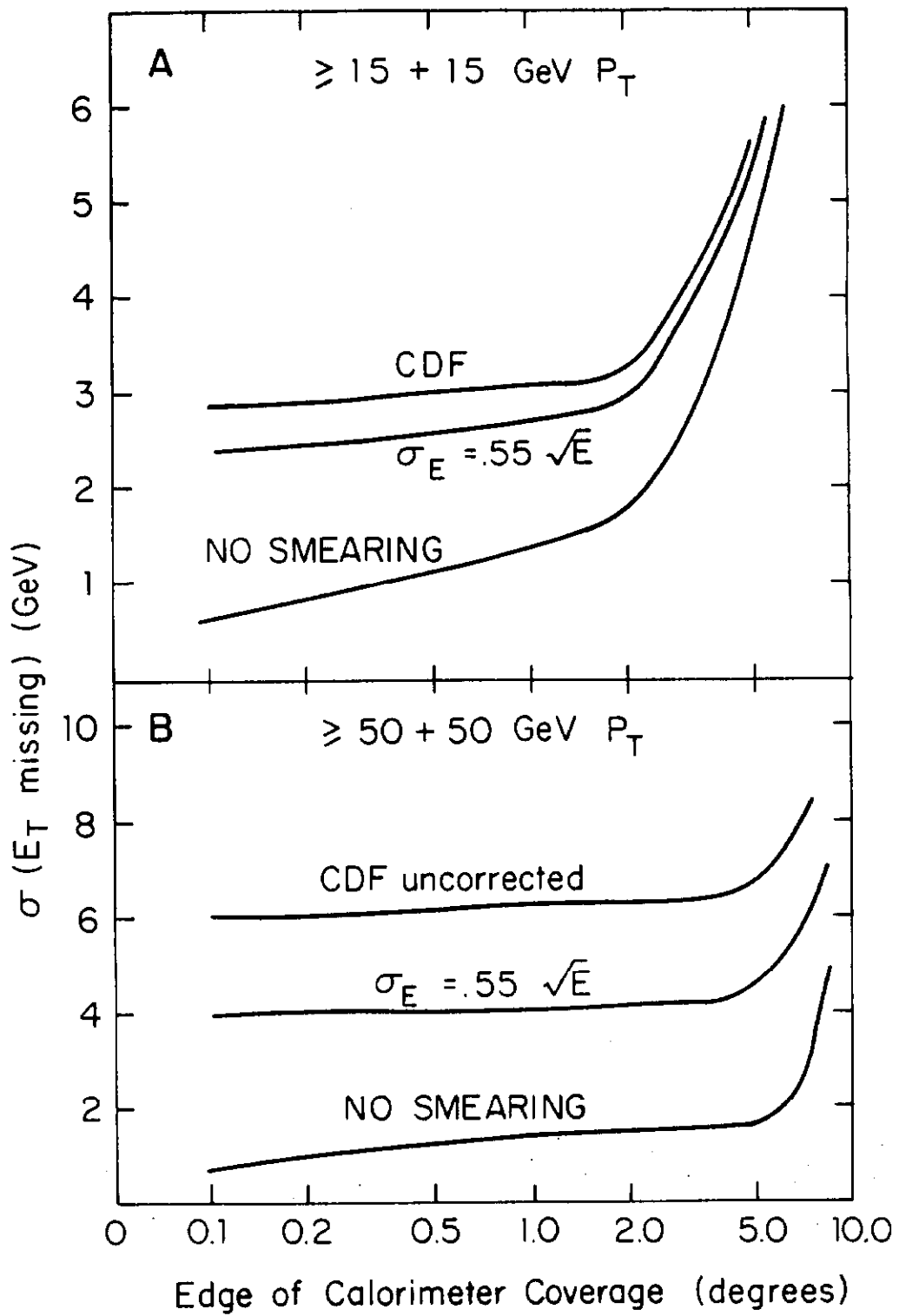


Fig. 1. Sigma of  $dN/dE_T$  missing versus size of half-cone of missing forward calorimetry

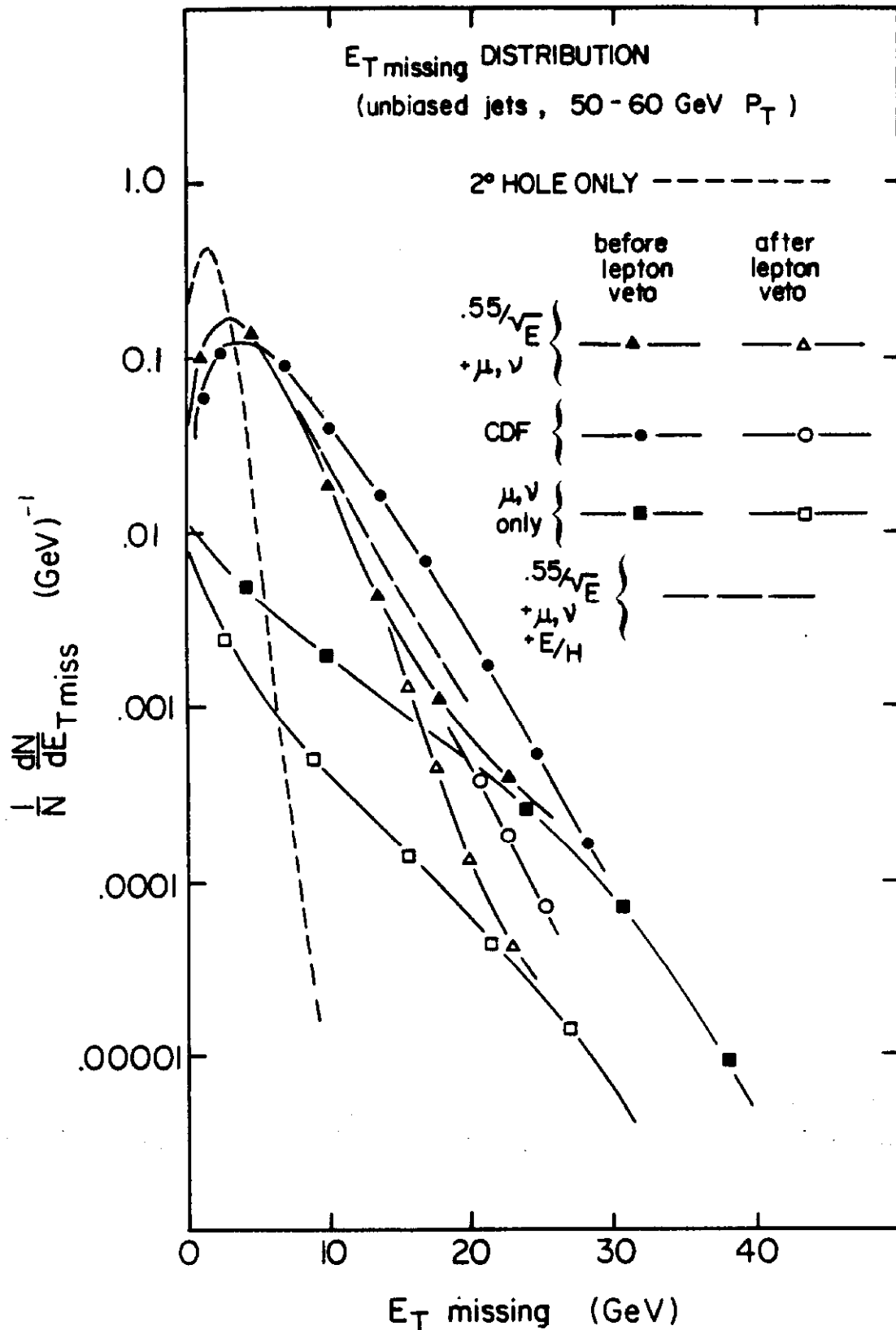


Fig. 2.  $1/N \frac{dN}{dE_T}$  missing for CDF, and "ideal" detectors with and without 2 GeV lepton veto. "Before lepton veto" curves have the same normalization. "After lepton veto" curves have normalization that reflects the reduction in number of events surviving the cut.

Fig. 3. Reconstructed mass fraction of  $w \rightarrow 2$  jets for "ideal" detectors with and without the effects of realistic clustering for jet definition.

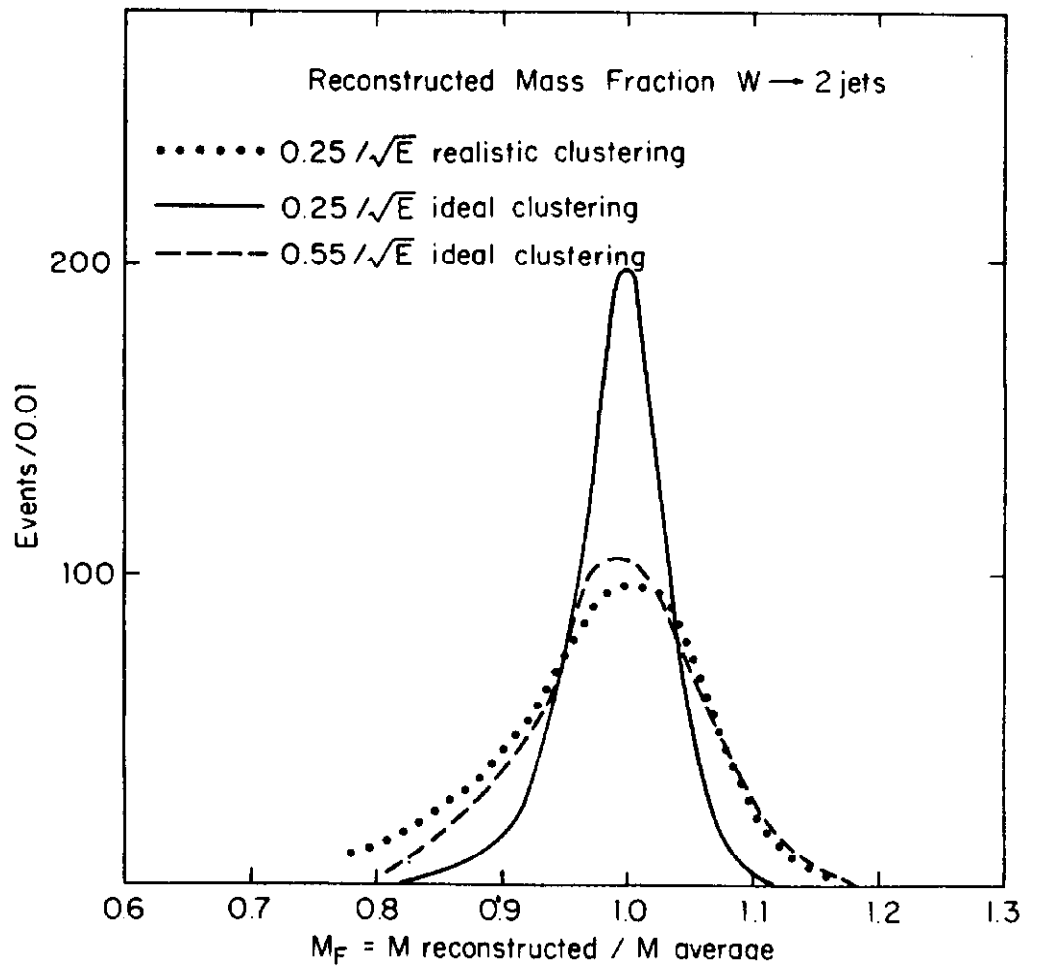


Fig. 4. Reconstructed mass fraction of  $w \rightarrow 2$  jets for CDF, "ideal" detectors including the effects of realistic clustering for jet definition.

